2022

Time-Dependent Alteration in the Chemoreflex Post-Acute Lung Injury

Kajal Kamra

Nikolay Karpuk

Ryan Adam

Irving H. Zucker

Harold D. Schultz

See next page for additional authors

Authors
Kajal Kamra, Nikolay Karpuk, Ryan Adam, Irving H. Zucker, Harold D. Schultz, and Han-Jun Wang

frontiers | Frontiers in Physiology

TYPE Original Research
PUBLISHED 20 October 2022
DOI 10.3389/fphys.2022.1009607

OPEN ACCESS

EDITED BY
Ying-Jie Peng,
The University of Chicago, United States

REVIEWED BY
David D. Kline,
University of Missouri, United States
Yee-Hsee Hsieh,
Case Western Reserve University, United States

*CORRESPONDENCE
Han-Jun Wang,
hanjunwang@unmc.edu

SPECIALTY SECTION
This article was submitted to Integrative Physiology, a section of the journal Frontiers in Physiology

RECEIVED 02 August 2022
ACCEPTED 04 October 2022
PUBLISHED 20 October 2022

CITATION
Kamra K, Karpuk N, Adam R, Zucker IH, Schultz HD and Wang H-J (2022), Time-dependent alteration in the chemoreflex post-acute lung injury. *Front. Physiol.* 13:1009607. doi: 10.3389/fphys.2022.1009607

Time-dependent alteration in the chemoreflex post-acute lung injury

Kajal Kamra[1,2], Nikolay Karpuk[2], Ryan Adam[1], Irving H. Zucker[1], Harold D. Schultz[1] and Han-Jun Wang[1,2]*

[1]Department of Cellular and Integrative Physiology, University of Nebraska Medical Center, Omaha, NE, United States, [2]Department of Anesthesiology, University of Nebraska Medical Center, Omaha, NE, United States

Acute lung injury (ALI) induces inflammation that disrupts the normal alveolar-capillary endothelial barrier which impairs gas exchange to induce hypoxemia that reflexively increases respiration. The neural mechanisms underlying the respiratory dysfunction during ALI are not fully understood. The purpose of this study was to investigate the role of the chemoreflex in mediating abnormal ventilation during acute (early) and recovery (late) stages of ALI. We hypothesized that the increase in respiratory rate (fR) during post-ALI is mediated by a sensitized chemoreflex. ALI was induced in male Sprague-Dawley rats using a single intra-tracheal injection of bleomycin (Bleo: low-dose = 1.25 mg/Kg or high-dose = 2.5 mg/Kg) (day 1) and respiratory variables- fR, V_t (Tidal Volume), and V_E (Minute Ventilation) in response to 10% hypoxia (10% O_2, 0% CO_2) and 5% hypercapnia/21% normoxia (21% O_2, 5% CO_2) were measured weekly from W0-W4 using whole-body plethysmography (WBP). Our data indicate sensitization (Δf_R = 93 ± 31 bpm, $p < 0.0001$) of the chemoreflex at W1 post-ALI in response to hypoxic/hypercapnic gas challenge in the low-dose bleo (moderate ALI) group and a blunted chemoreflex (Δf_R = −0.97 ± 42 bpm, $p < 0.0001$) at W1 post-ALI in the high-dose bleo (severe ALI) group. During recovery from ALI, at W3-W4, both low-dose and high-dose groups exhibited a sensitized chemoreflex in response to hypoxia and normoxic-hypercapnia. We then hypothesized that the blunted chemoreflex at W1 post-ALI in the high-dose bleo group could be due to near maximal tonic activation of chemoreceptors, called the "ceiling effect". To test this possibility, 90% hyperoxia (90% O_2, 0% CO_2) was given to bleo treated rats to inhibit the chemoreflex. Our results showed no changes in f_R, suggesting absence of the tonic chemoreflex activation in response to hypoxia at W1 post-ALI. These data suggest that during the acute stage of moderate (low-dose bleo) and severe (high-dose bleo) ALI, chemoreflex activity trends to be slightly sensitized and blunted, respectively while it becomes significantly sensitized during the recovery stage. Future studies are required to examine the molecular/cellular mechanisms underlying the time-course changes in chemoreflex sensitivity post-ALI.

KEYWORDS

acute lung injury, acute respiratory distress syndrome, bleomycin, chemoreceptors, chemoreflex, carotid bodies

Introduction

Acute lung injury (ALI) and its clinical correlate, the acute respiratory distress syndrome (ARDS), results due to disruption of the normal capillary endothelial barrier and invokes perturbations of ventilatory control (Young et al., 2019). Acute respiratory failure affects approximately 200,000 new cases each year in the US alone and accounts for 10% of ICU admissions with a high mortality and morbidity (Mowery et al., 2020). Current treatment therapies are focused on resolution of the lung disorder by fluid management, prone positioning, pharmacological interventions, and mechanical ventilation. ALI/ARDS causes marked diffuse alveolar damage, endothelial cell damage and pulmonary interstitial and alveolar edema that results in increased intrapulmonary shunt and dead space as well as atelectasis leading to a decreased functional lung size (Bernard et al., 1994; Ghio et al., 2001; Spinelli et al., 2020). This causes an impairment in gas exchange inducing hypoxemia, a hypoxic ventilatory response (HVR) and a reflexive increase in respiratory rate (f_R) (Bernard et al., 1994; Jacono et al., 2006; Spinelli et al., 2020). The neural mechanism that drives this increase in f_R during ALI is not fully understood.

Peripheral chemoreceptors in the carotid bodies (CBs) located at the bifurcation of the common carotid artery, are the first responders to hypoxia. A decrease in arterial pO_2 causes the glomus cells (type 1 cells) of the CBs to depolarize, increase intracellular calcium levels and closure of potassium channels to cause neurotransmitter release. The chemosensory afferent input from glomus cells then travels to the respiratory network in the brain stem through the carotid sinus nerve (CSN) which projects to the nucleus solitarius tractus (NTS) and respiratory motoneurons to induce a hypoxic ventilatory response (Sun et al., 1999; Prabhakar, 2000). The HVR in the early stage of ALI has been examined (Jacono et al., 2006; Huxtable et al., 2011) but little is known about the exact time-dependent changes in chemoreflex sensitivity in acute ALI and during the recovery of ALI. The specific objective of our study was to look at the time dependent respiratory changes in chemoreflex function in response to hypoxic and hypercapnic stimuli before ALI (Week 0; W0) and weekly for up to 4 weeks (W1-W4) post-ALI.

Methods

Ethical approval

Animals were housed in a temperature-controlled environment (22°C–25°C) with a 12 h light–dark cycle and *ad libitum* access to food and water, in accordance with standards set by the National Institutes of Health Guidelines for the Care and Use of Laboratory Animals. All experimental protocols were approved by the Institutional Animal Care and Use Committee (IACUC) of the University of Nebraska Medical Center (protocol ID no. 17-006-03 FC).

Animals

Thirty-three adult male Sprague-Dawley rats (2–3 months old) were used for these experiments. Animals were housed on-site in a controlled temperature environment (22°C–25°C) with a 12-h light-dark cycle and *ad libitum* access to food and water and were allowed to acclimate for 3 days to their new environment prior to the experiment. A small number of rats (1 high-dose bleo rat) died during experimentation after W2 post-bleo administration stemming from severe lung injury. All animal experimentation (collection of ventilatory parameters during rest and during hypoxic/hypercapnic gas exposure) was performed during the day (9.00–1600 h). Delivery of bleo (or saline) was

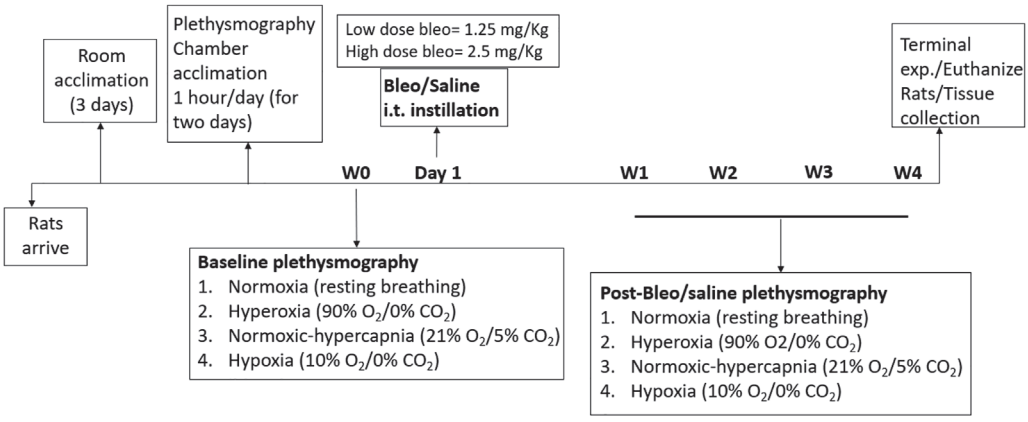

FIGURE 1
Timeline showing experimental design.

TABLE 1 Mean body weight and mean change in body weight (in grams) for sham, low-dose bleo and high-dose bleo rats.

	Mean body weight (grams)					Mean Δ body weight (grams)			
	W0	W1	W2	W3	W4	ΔW1	ΔW2	ΔW3	ΔW4
Sham (n = 14)	337 ± 41	405 ± 42***	443 ± 45****	472 ± 45****	485 ± 48****	69 ± 20	107 ± 27	136 ± 36	148 ± 35
Low-dose bleo (n = 10)	465 ± 114	472 ± 80	488 ± 66	506 ± 62	522 ± 55	6.6 ± 50	23 ± 60	41 ± 61	57 ± 65
High-dose bleo (n = 9)	301 ± 66	283 ± 71	313 ± 93	386 ± 65	412 ± 55ǂ	-19 ± 20	11 ± 56	77 ± 23	103 ± 21

Values are mean ± SD; One-way ANOVA with bonferroni multiple comparison test; bleo indicates bleomycin. ***p = 0.0004 (Sham-W0 vs. W1), ****p < 0.0001 (Sham- W0 vs. W2, W3 and W4), ǂp = 0.0117 (High-dose bleo- W0 vs. W4).

TABLE 2 Mean resting respiratory rate (f_R) (in BPM) for sham, low-dose bleo and high-dose bleo rats.

Mean resting f_R (BPM)					
	W0	W1	W2	W3	W4
Sham (n = 14)	108 ± 12	104 ± 15	107 ± 26	118 ± 25	99 ± 16
Low-dose bleo (n = 10)	97 ± 16	193 ± 55###	151 ± 41##	125 ± 31	103 ± 12
High dose-bleo (n = 9)	117 ± 21	333 ± 46ǂǂǂǂ	238 ± 81ǂǂ	198 ± 48ǂǂǂ	164 ± 47ǂǂ

Values are mean ± SD; One-way ANOVA with bonferroni multiple comparison test; f_R indicates respiratory rate; bleo indicates bleomycin. ##p = 0.007 (Low-dose bleo- W0 vs. W2), ###p = 0.001 (Low-dose bleo- W0 vs. W1), ǂǂp = 0.007 (High-dose bleo- W0 vs. W2), ǂǂp = 0.01 (High-dose bleo- W0 vs. W4), ǂǂǂp = 0.001 (High-dose bleo- W0 vs. W3), ǂǂǂǂp = 0.0001 (High-dose bleo- W0 vs. W1)

performed within our animal housing center. At the end of the experimental protocol, all animals were humanely euthanized with an overdose of pentobarbital sodium (150 mg/kg, IV). Euthanasia was confirmed by removal of vital organs and lung tissue was collected for further analysis. An experimental timeline is shown in Figure 1.

Drugs and chemicals

Bleomycin sulphate (bleo) was purchased from Enzo Life Sciences (New York, United States). Bleo was dissolved in saline for intra-tracheal administration. This procedure was performed within the animal housing center.

Rat model of lung injury

Rats were randomized into three experimental groups and lung parameters were measured at five time points- before (W0) and post-instillation (W1, 2, 3 and 4) as follows: sham rats (n = 14), low-dose bleo-treated rats (n = 10) and high-dose bleo-treated rats (n = 9). Bleo (2.5 mg/kg (high-dose) and 1.25 mg/kg (low-dose), ~0.15 ml) was instilled on day 1 intra-tracheally under 2%–3% isoflurane anesthesia. Sham control animals underwent intra-tracheal instillation of saline (~0.15 ml).

Breathing and ventilatory chemoreflex function at rest

Unrestrained whole-body plethysmography was utilized to measure ventilatory parameters- respiratory rate (f_R), tidal volume (V_t) and minute ventilation (V_E) in conscious rats by using signals from differential-pressure transducer (DLP 2.5, Harvard Apparatus), amplified and connected to PC *via* acquisition system PowerLab 35 Series managed by LabChart (v8.1.5) software (ADInstruments, Colorado, United States). Rats were acclimated to the plethysmograph chamber for 1 h each for two consecutive days prior to recordings. Respiratory parameters were not recorded during the acclimatization sessions. The plethysmograph chambers used for this study were custom-made (Midwest Plastics Inc., Nebraska, United States) and were 10, 10.5 and 20 cm in height, width, and length, respectively. The volume channel (i.e., flow integration) was calibrated by pushing 5 ml of air using a syringe before the start of the recording. During recordings, a constant flow of gas at 3 L/min was maintained to avoid an increase in humidity, temperature and CO_2 levels using a manually operated flow meter (Precision Medical, Northampton, PA, United States). Body weight (in grams) of rats was recorded prior to each experiment. In the resting state rats were exposed to normoxia (21% O_2, 0% CO_2) for baseline measurements followed by three different gas challenges- hyperoxia (90% O_2, 0% CO_2), hypoxia (10% O_2, 0% CO_2) and normoxic hypercapnia

10.3389/fphys.2022.1009607

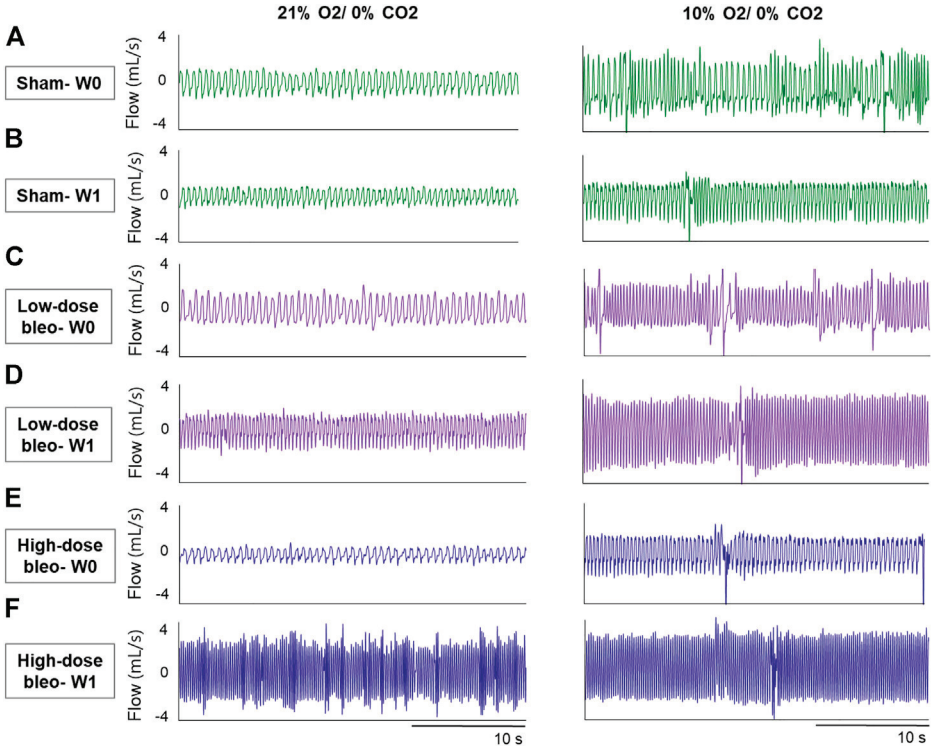

FIGURE 2
Representative recordings of resting breathing at normoxia (on left) and 10% hypoxia (on right) obtained in one rat per experimental group: **(A)** and **(B)** Sham (in green) at W0 and W1, respectively; **(C)** and **(D)** low-dose bleo (in purple) at W0 and W1, respectively; **(E)** and **(F)** high-dose bleo (in blue) at W0 and W1, respectively.

(21% O_2, 5% CO_2) balanced by N_2. The order of gas challenge was randomized and was maintained for 5 min. The last one-minute-long segment without any artifacts was used for analysis. A normoxic exposure of a minimum of 10 min or more was used in between challenges. All resting ventilatory parameters considered for analysis were recorded when the rats were awake and stationary (no activity-related events recorded in LabChart8 raw data file). V_E was calculated as the product of fR and V_t. V_t and V_E were normalized to bodyweight.

Statistical analysis

Data analysis in text, tables and figures are presented as mean ± SD. Statistical evaluation was analyzed using GraphPad Prism (GraphPad Software, San Diego, CA. Version 8). Comparisons between conditions (gas challenges) and for comparisons between groups (Sham, low-dose bleo and, high-dose bleo) repeated-measures two-way ANOVA with bonferroni corrections for multiple comparisons were used with $p < 0.05$ being statistically significant. For tables, the comparison of body weight and resting fR at each timepoint post-drug (bleo/saline) treatment with W0 (pre-treatment) within each experimental group was done using one-way ANOVA with bonferroni multiple comparison test with $p < 0.05$ being statistically significant.

Results

Effects of saline and bleomycin on body weight in rats

Body weights were measured weekly in all rats pre- (W0) and post-saline/bleo instillation (W1, 2, 3 and 4). At W1-post-bleo instillation, low-dose bleo-treated rats (Δ body weight at W1 post-ALI = 6.6 ± 50 g) showed no significant changes but high-dose bleo-treated rats (Δ body weight at W1 post-ALI = −19 ± 20 g) showed a reduction in body weight that was not statistically significant when compared to change in body weight in sham rats at W1-post-saline/bleo instillation (Δ body weight from W0 to W1 post-ALI = 69 ± 20 g) (Table 1). Sham and low-dose bleo-treated rats continued to gain weight each week throughout the experimental timeline (Table 1; Figure 1).

10.3389/fphys.2022.1009607

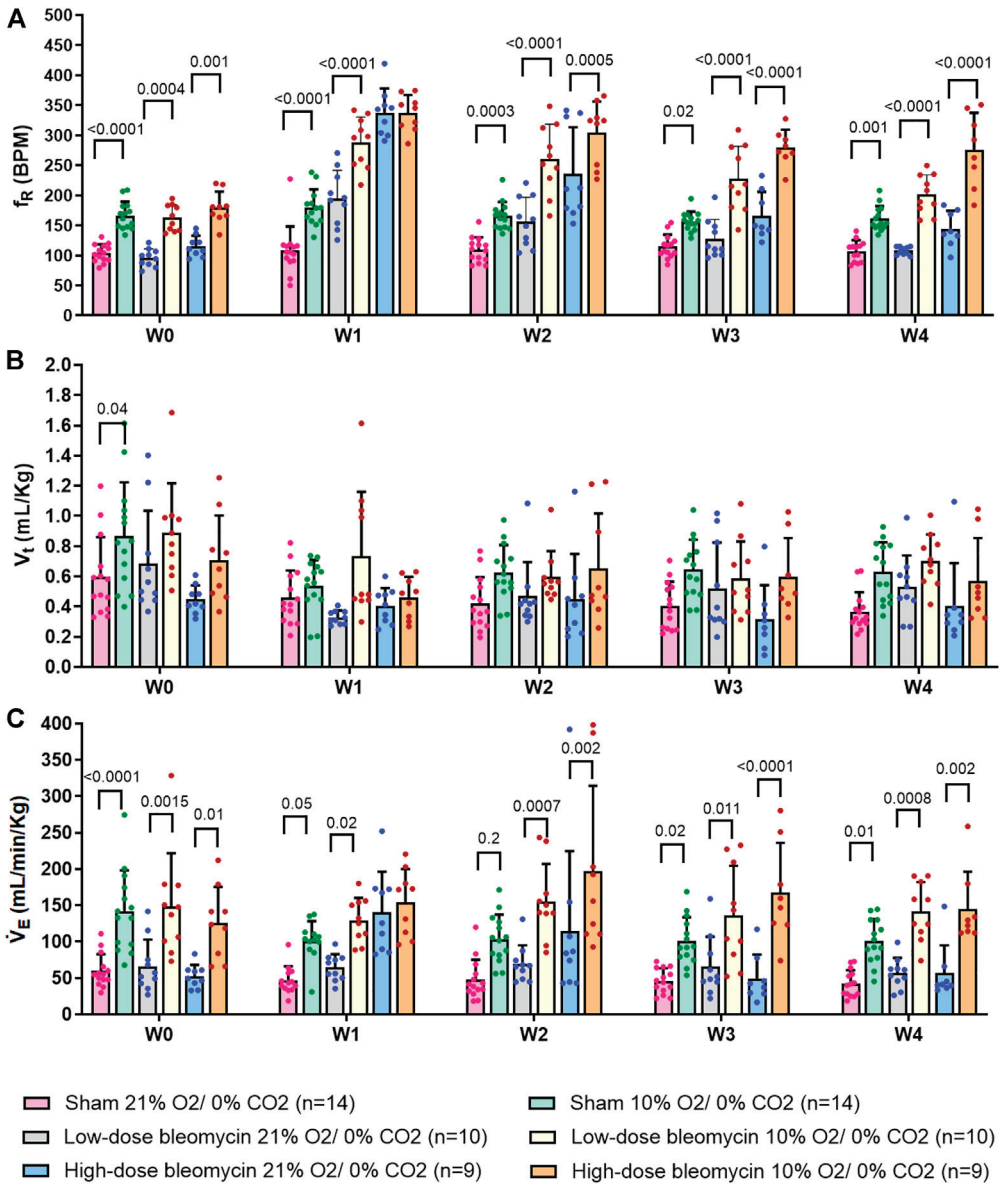

FIGURE 3
Effect of saline and (low-dose and high-dose) bleomycin on ventilatory parameters in sham (n = 14), low-dose bleo (n = 10) and high-dose bleo (n = 9) rats. Two-way ANOVA, Values are mean ± SD: **(A)** Respiratory rate (f_R) at normoxia vs. 10%; **(B)** Tidal volume (V_t) at normoxia vs. 10% hypoxia; **(C)** Minute ventilation (V_E) at normoxia vs. 10% hypoxia.

High-dose bleo-treated rats gained weight by the end of W3 and W4 (Table 1). One high dose bleo-treated rat died at W2.

Bleomycin caused an increase in resting f_R

As noted in Figures 2, 3A and Table 2 Sham rats showed a consistent normal resting f_R (180 ± 12 bpm) at W1 post-saline administration compared to W0 (104 ± 15 bpm). On the other hand, resting f_R increased ($p < 0.0001$) in both low-dose bleo- (193 ± 55 bpm) and high-dose bleo-treated rats (333 ± 46 bpm) at W1 post-bleo administration as compared to their baseline at W0 (low-dose group = 97 ± 16 bpm and high-dose group = 117 ± 21 bpm). The resting f_R in low- and high-dose bleo rats was partially restored by W3 (127 ± 32 bpm and 166 ± 40 bpm, respectively) and W4 (108 ± 7 bpm and 144 ± 30 bpm, respectively). These changes in resting f_R also influenced similar trends in resting V_E (Figures 3C, 4C). No significant changes were seen for the change in V_t in either group (Figures 3B and 4B).

10.3389/fphys.2022.1009607

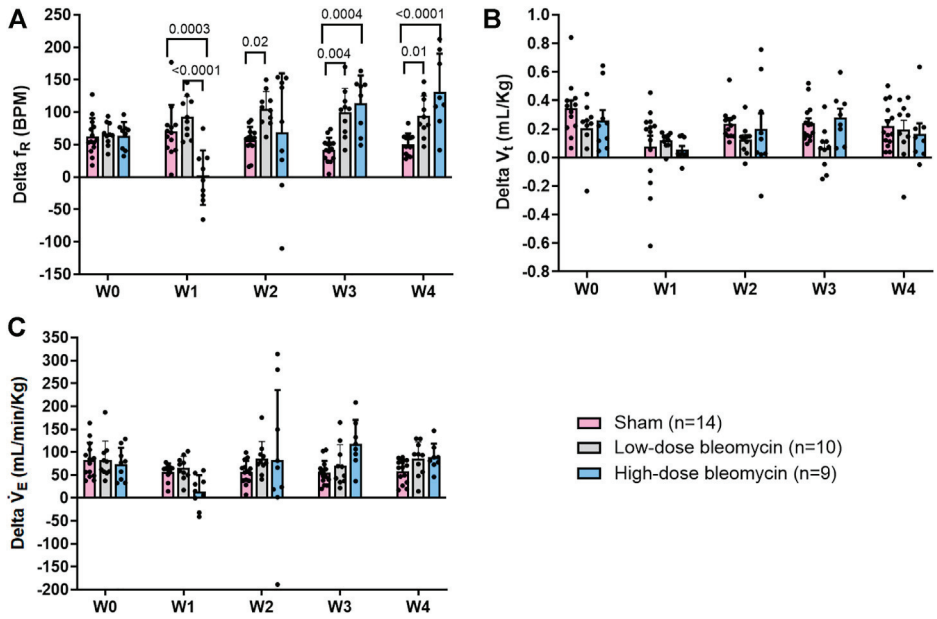

FIGURE 4
(A) Delta f_R; **(B)** Delta V_t; **(C)** Delta V_E in response to 10% hypoxia in sham (n = 14), low-dose bleo (n = 10) and high-dose bleo (n = 9) rats.

Effects of hypoxia on respiration

The peripheral chemoreflex was activated by challenging the rats with 10% hypoxia for a duration of 5 min and ventilatory parameters were assessed. The chemoreflex was assessed by measuring the absolute difference between 21% O_2/0% CO_2 and 10% O_2/0% CO_2. At baseline (W0), f_R increased in response to 10% O_2 in sham, low-dose and high-dose bleo-treated rats by 63 ± 29 bpm, 66 ± 18 bpm and 64 ± 21 bpm, respectively, before saline and bleo administration on day 1 (Figures 2A, 4A). 1W- post-saline/bleo administration, sham rats continued to respond normally to 10% hypoxic gas challenge. While the low-dose bleo-treated rats exhibited an activation of the chemoreflex with a significant increase in f_R (Δf_R = 93 ± 31 bpm, $p < 0.0001$). The high-dose bleo-treated rats, on the other hand, exhibited a significant blunting of the chemoreflex response (Δf_R = −0.97 ± 42 bpm, $p < 0.0001$) compared to sham rats with Δ f_R of 70 ± 41 bpm at 1W-post-bleo administration (Figures 2A, 4A).

For the high-dose bleo-treated rats, changes in V_E (ΔV_E) were not statistically significant (p = 0.8). However, we see a pattern of blunted ΔV_E at W1 (ΔV_E = 57 ± 18 ml/min/Kg and 14 ± 35 ml/min/Kg in sham and high-dose bleo-treated rats, respectively) due to a blunted Δf_R without significant changes in ΔV_t (Figure 4C). Sham rats continued to show a normal and consistent chemoreflex activation at W2 (Δf_R = 42 ± 19 bpm), W3 (Δf_R = 41 ± 19 bpm) and W4 (Δf_R = 50 ± 17 bpm). Low-dose bleo-treated rats exhibited an increased chemoreflex activation at W2 (Δf_R = 105 ± 26 bpm, p = 0.02) and a significant sensitization at W3 (Δf_R = 100 ± 37 bpm, p = 0.03) and at W4 (Δf_R = 94 ± 31 bpm, p = 0.006) when compared to the sham group for respective time points (Figure 4A). High-dose bleo-treated rats showed a restoration in chemoreflex activation at W2 (Δf_R = 69 ± 91 bpm) and show a chemoreflex sensitization at W3 (Δf_R = 114 ± 43 bpm, p = 0.007) and W4 (Δf_R = 132 ± 58 bpm, p = 0.001) when compared to the sham group for respective time points (Figure 4A). Similar trends were observed for ΔV_E in all experimental groups (Figure 4C). It is important to note that irrespective of the dose of bleomycin, there was sensitization of chemoreflex around W3 and 4. V_t was not significantly changed in either group (Figure 4B).

Effects of normoxic-hypercapnia on respiration

In the same groups of rats, both peripheral and central chemoreflexes were activated by challenging the rats with 5% CO_2/21% O_2 for a duration of 5 min. The chemoreflex was assessed by measuring the absolute difference between 21% O_2/0% CO_2 and 21% O_2/5% CO_2. At baseline (W0), f_R was increased in both sham and bleo-treated rats (low-dose and high-dose) by 62 ± 33 bpm, 66 ± 28 bpm and 63 ± 28 bpm before saline or bleo administration, respectively (Figures 5A, 6A). At W1 post-saline/bleo administration, sham rats continued to respond normally to 5% hypercapnic/21%

10.3389/fphys.2022.1009607

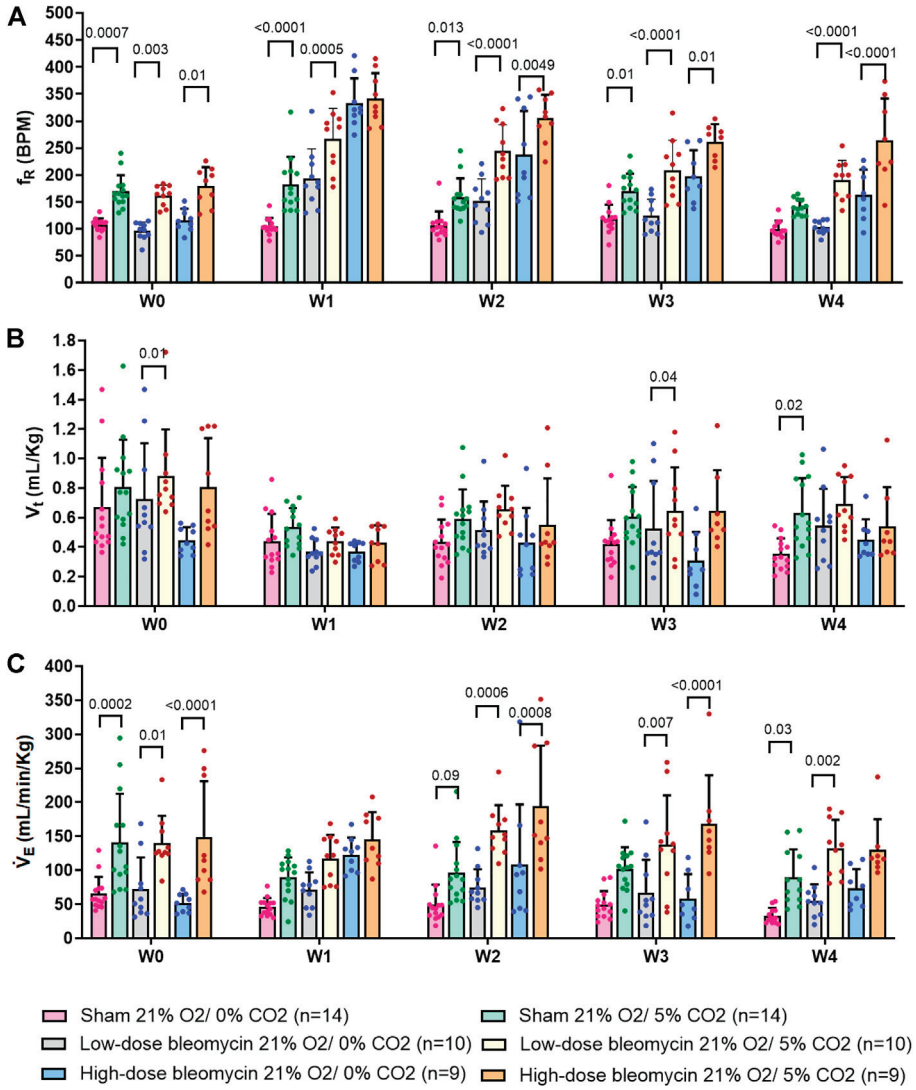

FIGURE 5
Effect of saline and (low-dose and high-dose) bleomycin on ventilatory parameters in sham (n = 14), low-dose bleo (n = 10) and high-dose bleo (n = 9) rats. Two-way ANOVA, Values are mean ± SD: **(A)** Respiratory rate (f_R) at normoxia vs. normoxic-hypercapnia; **(B)** Tidal volume (V_t) at normoxia and normoxic-hypercapnia; **(C)** Minute ventilation (V_E) at normoxia vs. normoxic-hypercapnia.

normoxic gas challenge (Δf_R = 77 ± 59 bpm). The low-dose bleo-treated rats exhibit a chemoreflex response to normoxic-hypercapnia (Δf_R = 74 ± 37 bpm) while the high-dose bleo-treated group showed a blunted chemoreflex response by a significant reduction in Δf_R to 8 ± 51 bpm (p = 0.004) compared to its timed-control (sham rats at W1) (Figure 6A). This blunted chemoreflex response was similar to the blunted peripheral chemoreflex response 1W post-bleo instillation.

Changes in ΔV_E showed a similar blunted pattern in bleo-treated rats at W1 (ΔV_E = 49 ± 25 ml/min/Kg, 46 ± 34 ml/min/Kg and 22 ± 40 ml/min/Kg in sham, low-dose, and high-dose bleo-treated rats, respectively) (Figures 5C and 6C) due to increased f_R without significant changes in V_t (Figures 5B and 6B) but were not statistically significant. Sham rats continued to show normal chemoreflex activation at W2 (Δf_R = 52 ± 32 bpm), W3 (53 ± 24 bpm) and W4 (42 ± 16 bpm). Although not statistically significant, low-dose bleo-treated rats showed a pattern of sensitized chemoreflex at W2 (93 ± 36 bpm), W3 (85 ± 35 bpm) and W4 (100 ± 92 bpm) just as seen for the peripheral chemoreflex in response to 10% hypoxia (Figure 6A). High-dose bleo-treated rats showed a restoration in chemoreflex activation at W2 (67 ± 71 bpm) and 3 (64 ± 35 bpm) and was sensitized at W4 (100 ± 92 bpm, p = 0.01) (Figure 6B). Similar trends were observed for ΔV_E in both experimental groups throughout the experimental timeline (Figure 6C).

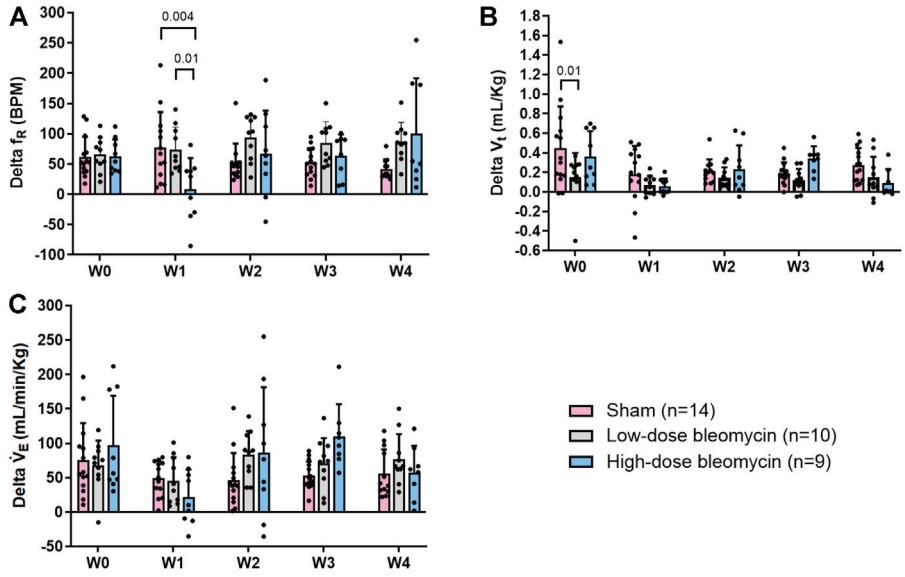

FIGURE 6
(A) Delta f_R; **(B)** Delta V_t; **(C)** Delta V_E in response to normoxic-hypercapnia in sham (n = 14), low-dose bleo (n = 10) and high-dose bleo (n = 9) rats.

Effects of hyperoxia on respiration 1-week post-bleo instillation

To inhibit tonic chemoreflex activation at rest, sham and bleo rats were exposed to 90% O_2/0% CO_2 gas mixture at W1 and ventilatory parameters were evaluated. No significant change in f_R was seen. (Figure 7A). 1W post-saline/bleo instillation (low- and high-dose), Δf_R for sham vs. low dose and high-dose bleo-treated rats was 8 ± 12 bpm, −4 ± 16 bpm and −6 ± 17 bpm, respectively (Figure 7B). No significant changes were seen for V_t in either group (Figures 7C,D). V_E was significantly higher in high-dose bleo group when compared to sham and low-dose bleo group (Figures 7E,F).

Discussion

The major findings of the present study are as follows: 1) both low-dose and high-dose bleo-treated rats showed a significant increase in resting f_R W1 post-bleo administration which was partially restored to normal by W3 and 4; 2) In response to 10% hypoxia and 5% normoxic-hypercapnia, while low-dose bleo-treated rats exhibited an activated peripheral chemoreflex response, the high-dose bleo-treated rats showed a blunted chemoreflex response at W1 post-bleo administration; 3) At W3 and 4, post-recovery from ALI, in response to 10% hypoxia and 5% normoxic-hypercapnia, both low-dose and high-dose bleo-treated rats exhibited a sensitized chemoreflex response; 4) In response to hyperoxia (90% O_2), both low-dose and high-dose treated bleo rats showed no significant reduction in the increased f_R at W1 post-bleo administration.

Shortness of breath and an increase in resting f_R caused by impairment of gas exchange are the main characteristics of ALI/ARDS which accounts for 10% of ICU admissions and has a high mortality rate (Mowery et al., 2020). Impaired gas exchange in ALI stimulates chemoreflex activation (Jacono et al., 2006). A time-course study of changes in chemoreflex activation during ALI has never been explored. The present study assesses the functional changes in chemoreflex activation over a 4-week time-course fashion from the beginning of ALI and during its recovery.

There are multiple ALI animal models reported in the scientific literature (Matute-Bello et al., 2008). However, no single model is the "best" model for ALI. We utilized the bleo model, which is widely used to model ALI (Moore and Hogaboam, 2008). Intra-tracheal administration of bleo damages the alveolar endothelium (Matute-Bello et al., 2008). Two different doses of bleo were used with the aim to study differences in the severity of ALI. Other common ALI animal models include the LPS model, which is also very reproducible and is widely used to study ALI (Zeng et al., 2017; Ye and Liu, 2020; Hou et al., 2021). Unfortunately, for the purpose of our current study, it could not be used because LPS is known to directly affect the sympathetic and parasympathetic ganglia (Shadiak et al., 1994; Hosoi et al., 2005; Kunda et al., 2014; Blum et al., 2017; Boucher et al., 2018) and for this reason, we think that LPS alone could directly

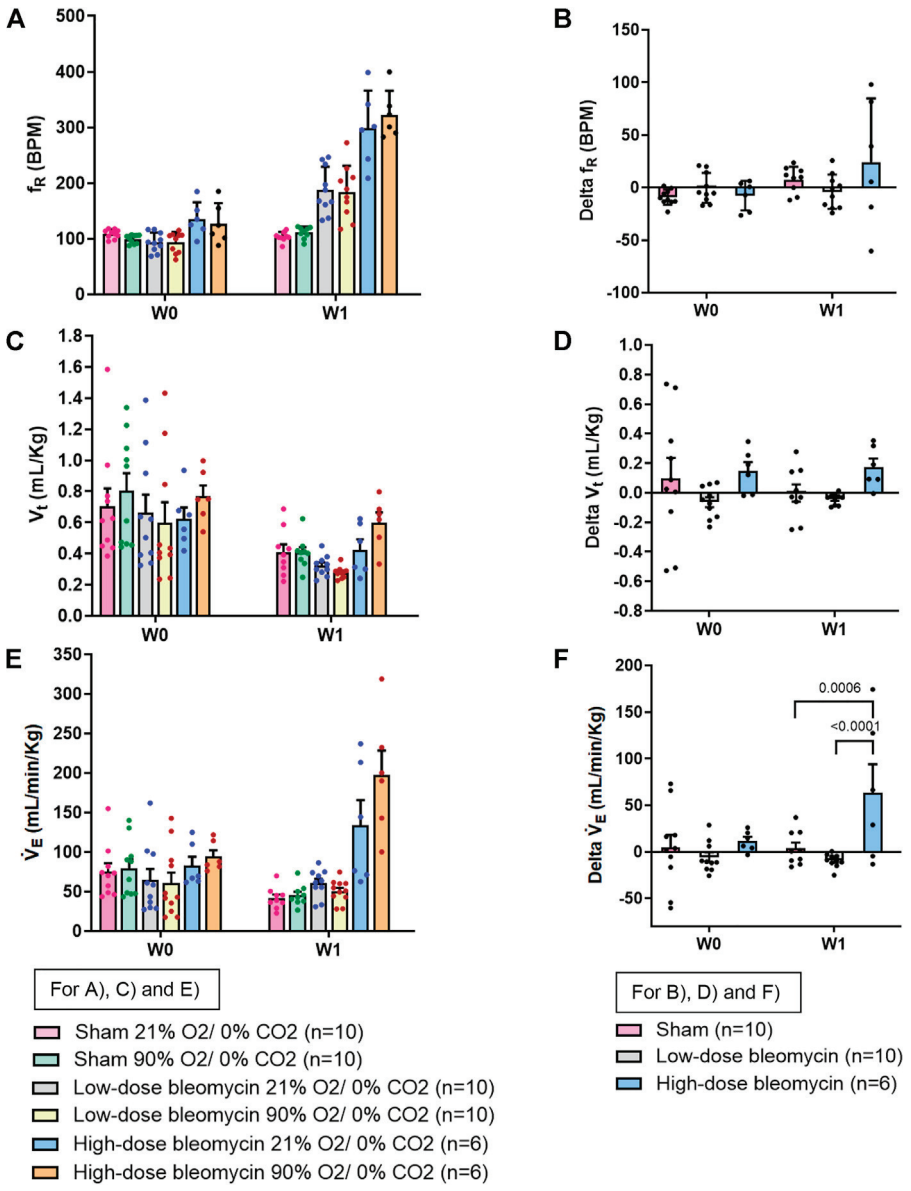

FIGURE 7
Effect of 90% hyperoxia on ventilatory parameters in sham (n = 10), low-dose bleo (n = 10) and high-dose bleo (n = 6) rats at W0 and W1. Two-way ANOVA, Values are mean ± SD: **(A)** Respiratory rate (f_R) at normoxia vs. 90% hyperoxia; **(B)** Delta f_R; **(C)** Tidal volume (V_t) at normoxia vs. 90% hyperoxia; **(D)** Delta V_t; **(E)** Minute ventilation (V_E) at normoxia and 90% hyperoxia; **(F)** Delta V_E.

interfere with the function of the carotid bodies thus confounding the primary goal of examining the effect of ALI on the chemoreflex.

Poor gas exchange caused by disruption of the normal alveolar-capillary endothelial barrier in this disease condition leads to systemic hypoxemia that is known to activate the peripheral chemoreceptors, which is one of the primary defense mechanisms to restore normal gas levels in the body (Dias-Freitas et al., 2016). Although there are some studies that provide possible mechanistic explanations but the neural mechanism(s) that drive the increase in f_R are not fully understood. The existing literature provides evidence that the chemoreflex function is altered during ALI (Jacono et al., 2006; Huxtable et al., 2011). A study by Jacono et al., 2006 showed that the chemoreflex, 5 days post-ALI, was sensitized in bleo-treated rats. This is consistent with what we see in our W1 post-low-dose bleo treated rats. Another study by Huxtable et al., 2012 used an LPS-ALI rat model to show an increase in resting f_R and a blunted chemoreflex response to 10.5% O_2, 7%CO_2 gas challenge at day 1 post-LPS

(i.p.) treatment. Our study showed that at W1 post-bleo treatment, while the low-dose bleo-treated rats exhibited a pattern of sensitized chemoreflex activity, the high-dose bleo-treated rats on the other hand exhibited a blunted chemoreflex response to 10% hypoxia. We initially thought that this may be possible due to a "ceiling effect", meaning that the chemoreflex could be maximally activated at baseline breathing normal (21% O_2) air. This possibility was ruled out by exposing the bleo-rats to hyperoxia with the goal to inhibit the chemoreflex (Figures 7A,B). Interestingly, we did not see a change in f_R in that group of rats. It is important to note that in this study, we are testing the chemoreflex activation in response to hypoxia, and both peripheral and central chemoreflex activation in response to normoxic-hypercapnia as a stimulus. We know that the CBs also get activated by changes in pH level which can act as a potential stimulus for chemoreflex activation in ALI condition. We have previously provided evidence that compared to vehicle-treated rats, bleo rats exhibit significantly decreased blood pO_2 and sO_2 at W1 post-bleo, indicating severe hypoxemia during acute lung injury. Bleo rats also exhibit elevated pCO_2 and decreased pH at W1 post-bleo, indicating blood acidosis (Kitzerow et al., 2022). Therefore, the role of other stimuli (such as, pH) in tonic activation of chemoreceptors during severe ALI condition require further investigation.

During the recovery from ALI, there was a partial restoration of the resting fR in bleo rats at W3 and W4. Histological proof of recovery from ALI post-intratracheal delivery of bleo has shown by many groups over the years (Moore and Hogaboam, 2008; Young et al., 2019; Mahmutovic Persson et al., 2020). Interestingly, at W3 and W4 post-ALI, the chemoreflex was sensitized in response to hypoxia and normoxic-hypercapnia in both low-dose- and high-dose bleo groups. We show for the first time to our knowledge, that chemoreflex activity during recovery from ALI is sensitized. The present study did not explore what causes the chemoreflex to be sensitized during recovery from ALI. It is possible that this may be attributed to multiple effects mediated at one or more levels of the reflex arc. Although the recovery phase of the ALI has not been extensively studied in terms of mechanisms for sensitized chemoreflex activity, it is already known that ALI influences both the pattern and the rhythm of breathing. In early stages of ALI (W1 post-bleo), Jacono et al. detected increased immunoreactivity of the pro-inflammatory cytokine interleukin-1β in the NTS from ALI rats. Bilateral micro-injections of IL-1β in the NTS of naïve rats showed increased f_R similar to that found in rats with ALI. They speculated that though initiated by sensory input, the characteristic ventilatory pattern after lung injury may be mediated by neuro-inflammation by cytokines in the NTS (Getsy et al., 2019; Hsieh et al., 2020; Litvin et al., 2020). Based on their evidence, it would not be surprising to expect similar plasticity in the NTS during the recovery stages of ALI. Our lab previously provided evidence of neuroinflammation and altered (increased) neuronal excitability in the stellate ganglia during the recovery phase of bleo-induced ALI (Hong et al., 2021). Based on this and our data for sensitized chemoreflex response to hypoxic stimulus, it is reasonable to speculate that similar neuroinflammation is possible in the carotid bodies which could lead to an altered chemoreflex function in this disease condition. In addition, a similar mechanism could also be possible in the superior cervical ganglion (SCG) that is located on the same sympathetic chain as the stellate ganglia. The post ganglionic axons of the SCG are known to innervate the CBs (Iturriaga et al., 2016). Electrical stimulation of the SCG has been shown to significantly sensitize the CB chemoreflex in hypertensive and normotensive rats (Felippe and Paton, 2021; Getsy et al., 2021; Felippe et al., 2022). Therefore, an increased SCG neuronal activity during the recovery of ALI, in-part, might also contribute to chemoreflex sensitization observed in our study. In addition, systemic hypoxia is a major consequence in chronic heart failure (CHF) condition (Morrissey et al., 2011) and studies provide evidence that experimental models of CHF (Andrade et al., 2015) and CHF patients (Giannoni et al., 2009) exhibit sensitized chemoreflex that contributes to sympatho-excitation and disordered breathing (Morrissey et al., 2011). Like CHF, ALI also leads to systemic hypoxia and a sensitized chemoreflex function in response to hypoxia. In addition, the increase in Ang II-dependent oxidative stress has been shown to contribute to altered CB function in CHF (Andrade et al., 2015). Interestingly, studies show that ALI results in decreased ACE2 expression and increased production of Ang II in the acid aspiration mice model of ALI (Imai et al., 2005). Therefore, Ang II signaling could be a potential mechanism causing sensitized chemoreflex during the recovery phase of ALI.

Conclusion

In summary, this study provides evidence that in the early phase of ALI, the chemoreflex is sensitized during low-dose ALI (moderate ALI) and blunted during high-dose bleo ALI (severe ALI). More importantly, it brings attention to the novel discovery of a sensitized chemoreflex during recovery from both moderate and severe ALI. The chemoreflexes are important modulators of sympathetic activation. It is well established that acute and/or chronic activation of the –chemoreflex enhances sympathetic drive (Plataki et al., 2013). Excessive sympathetic outflow can lead to cardiac arrythmias, cardio-renal syndrome, metabolic syndrome, T2 diabetes and deterioration of cardiac function (Paton et al., 2013; Conde et al., 2014; Iturriaga et al., 2016; Del Rio et al., 2017; Cunha-Guimaraes et al., 2020). Therefore, identification and further understanding of the neural mechanism that mediates changes in chemoreflex function during early and late stages of ALI will provide important

information for the long-term goal of development of novel targeted therapeutic approaches to improve clinical outcomes.

Data availability statement

The original contributions presented in the study are included in the article/Supplementary Material, further inquiries can be directed to the corresponding author.

Ethics statement

The animal study was reviewed and approved by the Institutional Animal Care and Use Committee (IACUC) of the University of Nebraska Medical Center.

Author contributions

KK, RA, and NK generated the data. KK analyzed the data and wrote the original draft manuscript. IZ, HS, and H-JW conceptually designed the study and reviewed, edited, and finalized the manuscript. All authors contributed to the article and approved the submitted version.

Funding

This study was supported by NIH grant R01 HL-152160 and in part, by NIH grants R01 HL-121012 and R01 HL126796. H-JW is also supported by Margaret R. Larson Professorship in Anesthesiology. IZ was partially supported by the Theodore F. Hubbard Foundation. KK is supported by American Heart Association predoctoral fellowship (ID:903872).

Conflict of interest

The authors declare that the research was conducted in the absence of any commercial or financial relationships that could be construed as a potential conflict of interest.

Publisher's note

All claims expressed in this article are solely those of the authors and do not necessarily represent those of their affiliated organizations, or those of the publisher, the editors and the reviewers. Any product that may be evaluated in this article, or claim that may be made by its manufacturer, is not guaranteed or endorsed by the publisher.

References

Andrade, D. C., Lucero, C., Toledo, C., Madrid, C., Marcus, N. J., Schultz, H. D., et al. (2015). Relevance of the carotid body chemoreflex in the progression of heart failure. *Biomed. Res. Int.* 2015, 467597. doi:10.1155/2015/467597

Bernard, G. R., ArtigAs, A., Brigham, K. L., Carlet, J., FalKe, K., Hudson, L., et al. (1994). The American-European Consensus Conference on ARDS. Definitions, mechanisms, relevant outcomes, and clinical trial coordination. *Am. J. Respir. Crit. Care Med.* 149 (3), 818–824. doi:10.1164/ajrccm.149.3.7509706

Blum, E., Procacci, P., Conte, V., Sartori, P., and HananiM. (2017). Long term effects of lipopolysaccharide on satellite glial cells in mouse dorsal root ganglia. *Exp. Cell Res.* 350 (1), 236–241. doi:10.1016/j.yexcr.2016.11.026

Boucher, Y., Moreau, N., Mauborgne, A., and Dieb, W. (2018). Lipopolysaccharide-mediated inflammatory priming potentiates painful post-traumatic trigeminal neuropathy. *Physiol. Behav.* 194, 497–504. doi:10.1016/j.physbeh.2018.06.021

Conde, S. V., Sacramento, J. F., Guarino, M. P., Gonzalez, C., Obeso, A., Diogo, L. N., et al. (2014). Carotid body, insulin, and metabolic diseases: Unraveling the links. *Front. Physiol.* 5, 418. doi:10.3389/fphys.2014.00418

Cunha-Guimaraes, J. P., Guarino, M. P., Timoteo, A. T., Caires, I., Sacramento, J. F., Ribeiro, M. J., et al. (2020). Carotid body chemosensitivity: Early biomarker of dysmetabolism in humans. *Eur. J. Endocrinol.* 182 (6), 549–557. doi:10.1530/EJE-19-0976

Del Rio, R., Andrade, D. C., Toledo, C., Diaz, H. S., Lucero, C., Arce-Alvarez, A., et al. (2017). Carotid body-mediated chemoreflex drive in the setting of low and high output heart failure. *Sci. Rep.* 7 (1), 8035–8110. doi:10.1038/s41598-017-08142-3

Dias-Freitas, F., Metelo-Coimbra, C., and Roncon-Albuquerque, R., Jr (2016). Molecular mechanisms underlying hyperoxia acute lung injury. *Respir. Med.* 119, 23–28. doi:10.1016/j.rmed.2016.08.010

Felippe, I., and Paton, J. (2021). Sympathetic control of carotid body sympathoexcitatory reflex responsiveness in spontaneously hypertensive rats. *FASEB J.* 35, 03247. doi:10.1096/fasebj.2021.35.s1.03247

Felippe, I. S., Zera, T., da Silva, M. P., Moraes, D. J. A., McBryde, F., and Paton, J. F. R. (2022). The sympathetic nervous system exacerbates carotid body sensitivity in hypertension. *Cardiovasc. Res.* 2022, cvac008. doi:10.1093/cvr/cvac008

Getsy, P. M., Coffee, G. A., Hsieh, Y. H., and Lewis, S. J. (2021). Loss of cervical sympathetic chain input to the superior cervical ganglia affects the ventilatory responses to hypoxic challenge in freely-moving C57BL6 mice. *Front. Physiol.* 12, 619688. doi:10.3389/fphys.2021.619688

Getsy, P. M., Mayer, C. A., MacFarlane, P. M., Jacono, F. J., and Wilson, C. G. (2019). Acute lung injury in neonatal rats causes postsynaptic depression in nucleus tractus solitarii second-order neurons. *Respir. Physiol. Neurobiol.* 269, 103250. doi:10.1016/j.resp.2019.103250

Ghio, S., GavAzzi, A., Campana, C., Inserra, C., Klersy, C., Sebastiani, R., et al. (2001). Independent and additive prognostic value of right ventricular systolic function and pulmonary artery pressure in patients with chronic heart failure. *J. Am. Coll. Cardiol.* 37 (1), 183–188. doi:10.1016/s0735-1097(00)01102-5

Giannoni, A., Emdin, M., Bramanti, F., Iudice, G., Francis, D. P., Barsotti, A., et al. (2009). Combined increased chemosensitivity to hypoxia and hypercapnia as a prognosticator in heart failure. *J. Am. Coll. Cardiol.* 53 (21), 1975–1980. doi:10.1016/j.jacc.2009.02.030

Hong, J., Adam, R. J., Gao, L., Hahka, T., Xia, Z., Wang, D., et al. (2021). Macrophage activation in stellate ganglia contributes to lung injury-induced arrhythmogenesis in male rats. *Acta Physiol.* 232 (2), e13657. doi:10.1111/apha.13657

Hosoi, T., Okuma, Y., Matsuda, T., and Nomura, Y. (2005). Novel pathway for LPS-induced afferent vagus nerve activation: Possible role of nodose ganglion. *Auton. Neurosci.* 120 (1-2), 104–107. doi:10.1016/j.autneu.2004.11.012

Hou, L., Zhang, J., Liu, Y., Fang, H., Liao, L., Wang, Z., et al. (2021). MitoQ alleviates LPS-mediated acute lung injury through regulating Nrf2/Drp1 pathway. *Free Radic. Biol. Med.* 165, 219–228. doi:10.1016/j.freeradbiomed.2021.01.045

Hsieh, Y. H., Litvin, D. G., Zaylor, A. R., Nethery, D. E., Dick, T. E., and Jacono, F. J. (2020). Brainstem inflammation modulates the ventilatory pattern and its

variability after acute lung injury in rodents. *J. Physiol.* 598 (13), 2791–2811. doi:10.1113/JP279177

Huxtable, A., Vinit, S., Windelborn, J. A., Crader, S. M., Guenther, C. H., Watters, J. J., et al. (2011). Systemic inflammation impairs respiratory chemoreflexes and plasticity. *Respir. Physiol. Neurobiol.* 178 (3), 482–489. doi:10.1016/j.resp.2011.06.017

Imai, Y., Kuba, K., Rao, S., Huan, Y., Guo, F., Guan, B., et al. (2005). Angiotensin-converting enzyme 2 protects from severe acute lung failure. *Nature* 436 (7047), 112–116. doi:10.1038/nature03712

Iturriaga, R., Rio, R. D., Idiaquez, J., and Somers, V. K. (2016). Carotid body chemoreceptors, sympathetic neural activation, and cardiometabolic disease. *Biol. Res.* 49, 13. doi:10.1186/s40659-016-0073-8

Jacono, F. J., Peng, Y. J., Nethery, D., Faress, J. A., Lee, Z., Kern, J. A., et al. (2006). Acute lung injury augments hypoxic ventilatory response in the absence of systemic hypoxemia. *J. Appl. Physiol.* 101 (6), 1795–1802. doi:10.1152/japplphysiol.00100.2006

Kitzerow, O., Zucker, I. H., Lisco, S. J., and Wang, H. J. (2022). Timeline of multi-organ plasma extravasation after bleomycin-induced acute lung injury. *Front. Physiol.* 13, 777072. doi:10.3389/fphys.2022.777072

Kunda, P. E., Cavicchia, J. C., and Acosta, C. G. (2014). Lipopolysaccharides and trophic factors regulate the LPS receptor complex in nodose and trigeminal neurons. *Neuroscience* 280, 60–72. doi:10.1016/j.neuroscience.2014.08.053

Litvin, D. G., Denstaedt, S. J., Borkowski, L. F., Nichols, N. L., Dick, T. E., Smith, C. B., et al. (2020). Peripheral-to-central immune communication at the area postrema glial-barrier following bleomycin-induced sterile lung injury in adult rats. *Brain Behav. Immun.* 87, 610–633. doi:10.1016/j.bbi.2020.02.006

Mahmutovic Persson, I., Falk Hakansson, H., Orbom, A., Liu, J., von Wachenfeldt, K., and Olsson, L. E. (2020). Imaging biomarkers and pathobiological profiling in a rat model of drug-induced interstitial lung disease induced by bleomycin. *Front. Physiol.* 11, 584. doi:10.3389/fphys.2020.00584

Matute-Bello, G., Frevert, C. W., and Martin, T. R. (2008). Animal models of acute lung injury. *Am. J. Physiol. Lung Cell. Mol. Physiol.* 295 (3), L379–L399. doi:10.1152/ajplung.00010.2008

Moore, B. B., and Hogaboam, C. M. (2008). Murine models of pulmonary fibrosis. *Am. J. Physiol. Lung Cell. Mol. Physiol.* 294 (2), L152–L160. doi:10.1152/ajplung.00313.2007

Morrissey, R. P., Czer, L., and Shah, P. K. (2011). Chronic heart failure: Current evidence, challenges to therapy, and future directions. *Am. J. Cardiovasc. Drugs* 11 (3), 153–171. doi:10.2165/11592090-000000000-00000

Mowery, N. T., Terzian, W. H., and Nelson, A. C. (2020). Acute lung injury. *Curr. Probl. Surg.* 57 (5), 100777. doi:10.1016/j.cpsurg.2020.100777

Paton, J. F., Sobotka, P. A., Fudim, M., Engelman, Z. J., Engleman, Z. J., Hart, E. C. J., et al. (2013). The carotid body as a therapeutic target for the treatment of sympathetically mediated diseases. *Hypertension* 61 (1), 5–13. doi:10.1161/HYPERTENSIONAHA.111.00064

Plataki, M., Sands, S. A., and Malhotra, A. (2013). Clinical consequences of altered chemoreflex control. *Respir. Physiol. Neurobiol.* 189 (2), 354–363. doi:10.1016/j.resp.2013.04.020

Prabhakar, N. R. (2000). Oxygen sensing by the carotid body chemoreceptors. *J. Appl. Physiol.* 88 (6), 2287–2295. doi:10.1152/jappl.2000.88.6.2287

Shadiak, A. M., Carlson, C. D., DingM.Hart, R. P., and Jonakait, G. M. (1994). Lipopolysaccharide induces substance P in sympathetic ganglia via ganglionic interleukin-1 production. *J. Neuroimmunol.* 49 (1-2), 51–58. doi:10.1016/0165-5728(94)90180-5

Spinelli, E., Mauri, T., Beitler, J. R., Pesenti, A., and Brodie, D. (2020). Respiratory drive in the acute respiratory distress syndrome: Pathophysiology, monitoring, and therapeutic interventions. *Intensive Care Med.* 46 (4), 606–618. doi:10.1007/s00134-020-05942-6

Sun, S.-Y., Wang, W., Zucker, I. H., and Schultz, H. D. (1999). Enhanced peripheral chemoreflex function in conscious rabbits with pacing-induced heart failure. *J. Appl. Physiol.* 86 (4), 1264–1272. doi:10.1152/jappl.1999.86.4.1264

Ye, R., and Liu, Z. (2020). ACE2 exhibits protective effects against LPS-induced acute lung injury in mice by inhibiting the LPS-TLR4 pathway. *Exp. Mol. Pathol.* 113, 104350. doi:10.1016/j.yexmp.2019.104350

Young, B. P., Loparo, K. A., Dick, T. E., and Jacono, F. J. (2019). Ventilatory pattern variability as a biometric for severity of acute lung injury in rats. *Respir. Physiol. Neurobiol.* 265, 161–171. doi:10.1016/j.resp.2019.03.009

Zeng, M., Sang, W., Chen, S., Chen, R., Zhang, H., Xue, F., et al. (2017). 4-PBA inhibits LPS-induced inflammation through regulating ER stress and autophagy in acute lung injury models. *Toxicol. Lett.* 271, 26–37. doi:10.1016/j.toxlet.2017.02.023